Clinical Cancer Research

ABBV-399, a c-Met Antibody–Drug Conjugate that Targets Both *MET*–Amplified and c-Met–Overexpressing Tumors, Irrespective of *MET* Pathway Dependence

Jieyi Wang[1], Mark G. Anderson[1], Anatol Oleksijew[1], Kedar S. Vaidya[1], Erwin R. Boghaert[1], Lora Tucker[1], Qian Zhang[1], Edward K. Han[1], Joann P. Palma[1], Louie Naumovski[2], and Edward B. Reilly[1]

Abstract

Purpose: Despite the importance of the *MET* oncogene in many malignancies, clinical strategies targeting c-Met have benefitted only small subsets of patients with tumors driven by signaling through the c-Met pathway, thereby necessitating selection of patients with *MET* amplification and/or c-Met activation most likely to respond. An ADC targeting c-Met could overcome these limitations with potential as a broad-acting therapeutic.

Experimental Design: ADC ABBV-399 was generated with the c-Met–targeting antibody, ABT-700. Antitumor activity was evaluated in cancer cells with overexpressed c-Met or amplified *MET* and in xenografts including patient-derived xenograft (PDX) models and those refractory to other c-Met inhibitors. The correlation between c-Met expression and sensitivity to ABBV-399 in tumor and normal cell lines was assessed to evaluate the risk of on-target toxicity.

Results: A threshold level of c-Met expressed by sensitive tumor but not normal cells is required for significant ABBV-399–mediated killing of tumor cells. Activity extends to c-Met or amplified *MET* cell line and PDX models where significant tumor growth inhibition and regressions are observed. ABBV-399 inhibits growth of xenograft tumors refractory to other c-Met inhibitors and provides significant therapeutic benefit in combination with standard-of-care chemotherapy.

Conclusions: ABBV-399 represents a novel therapeutic strategy to deliver a potent cytotoxin to c-Met–overexpressing tumor cells enabling cell killing regardless of reliance on *MET* signaling. ABBV-399 has progressed to a phase I study where it has been well tolerated and has produced objective responses in c-Met–expressing non–small cell lung cancer (NSCLC) patients.
Clin Cancer Res; 23(4); 992–1000. ©2016 AACR.

Introduction

The c-Met receptor tyrosine kinase is the cell surface receptor for hepatocyte growth factor (HGF) encoded by the *MET* proto-oncogene (1). The c-Met/HGF axis is aberrantly activated in multiple cancers through *MET* genomic amplification, transcriptional upregulation and ligand-dependent mechanisms, thereby contributing to tumor progression, angiogenesis, invasive growth, metastasis, and resistance to therapies (1). The development of c-Met/HGF axis inhibitors, both antibodies and small molecules, has been an active area of cancer research (2–4). The development of c-Met–directed therapeutic antibodies has been hampered by the induction of agonistic activity (5, 6). The resulting approach to c-Met–directed therapeutic antibody development has, therefore, focused on the "one-armed" antibody (onartuzumab; Roche) or antibodies to the HGF ligand (rilotumumab; Amgen; 7–9). Small-molecule inhibitors of c-Met signaling have also been developed (e.g., cabozatinib, Exelixis; crizotinib, Pfizer; tivantinib, ArQule) although many of these are nonselective broad-spectrum kinase inhibitors that may or may not directly target c-Met (10–13).

Although several of these inhibitors have advanced into clinical trials, results with this drug class did not induce demonstrable survival benefit (14, 15). Scrutiny of these trial outcomes suggests that c-Met expression on tumors by itself is not a sufficient predictor for activity. Instead patient selection strategies to identify those tumors in which *MET* is constitutively activated through gene amplification, mutation, or ligand-dependent activation may be necessary to predict sensitivity to many of these inhibitors (14, 15). Consistent with reliance on *MET* activation for activity, ABT-700, a c-Met–targeting antibody without the agonist activity associated with many c-Met antibodies, was well tolerated in a phase I trial and demonstrated antitumor activity in select patients with *MET*-amplified solid tumors (16, 17). Although increased frequencies of *MET* amplification may be associated with relapsed/refractory tumors including those with EGFR-activating

[1]AbbVie, Oncology Discovery, North Chicago, Illinois. [2]AbbVie Biotherapeutics Research, Redwood City, California.

Note: Supplementary data for this article are available at Clinical Cancer Research Online (http://clincancerres.aacrjournals.org/).

J. Wang and M.G. Anderson contributed equally to this article.

Current address for J. Wang: Lyvgen Biopharma, 67-4 Libin Road, Zhangjiang Hi-tech District, Shanghai 201203, China.

Corresponding Author: Edward B. Reilly, AbbVie, Oncology Discovery, R460, 1 North Waukegan Road, North Chicago, IL 60064-6099. Phone: 847-937-0815; Fax: 847-938-1336; E-mail: ed.reilly@abbvie.com

doi: 10.1158/1078-0432.CCR-16-1568

Translational Relevance

The antitumor activity of c-Met inhibitors is generally limited to tumors that are *MET*-activated and driven predominately by c-Met signaling. ABBV-399, a c-Met targeting ADC, represents a novel therapeutic delivering a potent cytotoxin to c-Met–overexpressing tumor cells enabling cell killing regardless of reliance on *MET* signaling. ABBV-399 treatment, alone and in combination with standard-of-care chemotherapy, induces significant tumor growth inhibition and regressions in tumor cell line and PDX models with overexpressed c-Met or amplified *MET* including tumors refractory to other c-Met inhibitors. We demonstrate ABBV-399 killing requires a threshold level of c-Met, expressed by sensitive tumor but not normal cells. These data indicate that ABBV-399 may be an effective broad-acting c-Met–targeting therapeutic that can overcome limitations associated with other c-Met inhibitors. ABBV-399 has progressed to a phase I study where it has been well tolerated and has produced objective responses in c-Met–expressing NSCLC patients.

mutation in non–small cell lung cancer (NSCLC), primary *MET* genomic amplification is a low frequency event in most tumors (1%–5%), thereby limiting the patient population where inhibitors that block *MET* signaling may be effective (18–21).

An ADC targeting c-Met represents an attractive therapeutic strategy that does not depend on downstream signaling for efficacy but rather on target expression. If successful, this approach could expand the breadth of treatment beyond that attainable with other c-Met inhibitors as c-Met overexpression occurs in 30%–50% of solid tumors, including NSCLC, colorectal cancer and advanced gastroesophageal cancer (22–24). ABBV-399 is an ADC comprised of the ABT-700 antibody conjugated to the clinically validated cytotoxic microtubule inhibitor monomethylauristatin E (MMAE) via a cleavable valine–citrulline (vc) linker (25, 26). Although a c-Met–targeting ADC presents the risk of on-target toxicity based on c-Met normal tissue expression, c-Met expression is significantly higher in many cancers compared with normal tissues (27–31) suggesting that a therapeutic window may exist for a selectively targeting ADC. We investigated the preclinical characteristics of ABBV-399 including its antitumor activity against a variety of c-Met–overexpressed, *MET*-amplified, and c-Met inhibitor–refractory tumor models. Collectively, these results provided the basis for advancing ABBV-399 to phase I studies in patients with c-Met overexpression where objective responses have been observed (32).

Materials and Methods

Antibodies and reagents

ABT-700, an anti-human c-Met–targeting antibody derived from the mAb 224G11 was produced from a stable transfected stable CHO cell line as described previously (12). ABBV-399 was generated from the conjugation of vc MMAE to interchain disulfide bonds in ABT-700 after mild reduction to the sulfhydryl group (25). The average drug:antibody ratio of ABBV-399 was approximately 3.1. Recombinant human c-Met extracellular domain with a His tag (rh-c-Met ECD-6His) was expressed in and purified from HEK293 cells. HGF was purchased from R&D Systems. 5-Fluorouracil (APP Pharmaceuticals) and irinotecan (Hospira) were obtained as solutions and diluted with 0.9% NaCl for injection (USP), and leucovorin calcium (Fluka Chemical) was obtained as a salt and reconstituted with saline before dosing.

Cell culture

The tumor cell lines A549, Hs 746T, SW-48, HT-29, MDA-MB-231, MCF-7, U-87-MG, and IM-95 were obtained from ATCC and maintained in DMEM (Life Technologies) supplemented with 10% FBS (HyClone). All cells were cultured in a humidified, 5% CO_2 environment; EBC-1 was obtained from the JCRB Cell Bank; IM-95 was supplemented with 10 mg/L insulin (Sigma). NCI-H1573, NCI-H820, NCI-H441, NCI-H1650, SNU-620, and SNU-5 were obtained from ATCC and maintained in RPMI (Life Technologies) supplemented with 10% FBS. The NCI-H1573, EBC-1, Hs 746T, SNU-620, and SNU-5 tumor cell lines were previously shown to harbor *MET* gene amplification (17). KP4 cells were obtained from RIKEN (Riken BioResource Center) and cultured in DMEM and 10% FBS. Nontransformed cell lines NHBE (CC-3170), HUVEC (CC-3162, EGM-2), HMEC (CC-3150), PrEC (CC-3166), and NHDF (CC-3132) were obtained from Lonza and cultured using manufacturer recommended conditions.

All cell lines were expanded in culture upon receipt and cryopreserved to provide cells at a similar stage passage for all subsequent experiments. All cell lines were authenticated; however, for cell lines not authenticated in the 6 months before use, their c-Met expression levels were confirmed by FACS analysis.

Binding ELISA and FACS analysis

Binding ELISA was performed as described previously (17). For cellular c-Met–binding studies, cells were harvested from flasks when approximately 80% confluent using Cell Dissociation Buffer (Life Technologies). Cells were washed once in PBS/1% FBS (FACS buffer), resuspended at 1.5–2 $\times$ 10^6 cells/mL in FACS buffer and transferred to a round-bottom 96-well plate Corning Life Sciences) at 100 μL/well. Ten microliters of a 10$\times$ concentration of ABT-700, ABBV-399, or controls were added and plates were incubated at 4°C for 2 hours. Wells were washed twice with FACS buffer and resuspended in 50 μL of 1:500 anti-human IgG Ab (AlexaFluor 488, Invitrogen) diluted in FACS buffer. Plates were incubated at 4°C for 1 hour, washed twice with FACS buffer. Cells were resuspended in 100 μL of PBS/1% formaldehyde and analyzed on a Becton Dickinson LSRII flow cytometer.

Determination of receptor density

c-Met cell surface density (antigen-binding capacity per cell) was determined by indirect immunofluorescence staining of cell surface antigens on cultured cells using QIFIKIT (Dako). Briefly, cells were harvested from a culture flask as described above for FACS analysis, added to a round-bottom 96-well plate at 100 μL/well, and incubated at 4°C with 3 μg/mL c-Met antibody m224G11 (the murine parent antibody of ABT-700). Wells treated with an irrelevant mouse mAb of the same isotype mIgG1 at 3 μg/mL were included as controls. Following a 1-hour incubation with primary antibody, cells were centrifuged for 3 minutes at 300 $\times$ *g*, washed twice with FACS buffer, and incubated for 1 hour at 4°C with 100 μL of the QIFIKIT-provided FITC-conjugated antibody diluted 1:50 in FACS buffer. Cells were centrifuged for 3 minutes at 300 $\times$ *g*, washed twice with FACS buffer, and fixed

with 100 μL/well of 1% formaldehyde in PBS. Indirect immunofluorescence staining of the QIFIKIT beads were carried out according to the manufacturer's instructions and data were acquired on a Becton Dickinson LSRII flow cytometer. The standard curve was used to assign ABC (antibody-binding capacity) or number of receptors for each cell line.

IHC

Immunohistochemical staining was performed on 4-μm sections using the CONFIRM anti-c-Met (SP44) rabbit monoclonal primary antibody (Ventana Medical Systems) on the Ventana Benchmark Ultra Autostainer according to the manufacturer's protocol. Briefly, antigen retrieval was performed by placing unstained slides in Ventana Ultra CC1 buffer (Tris-EDTA/EGTA, pH 9) at 64°C for 95 minutes followed by incubation of tissues with the primary antibody (SP44) at 36°C for 16 minutes. Antigen–antibody reaction was visualized using the Ultraview Universal DAB Detection Kit. Hematoxylin staining for 8 minutes followed by a bluing reagent (Ventana Medical Systems) for 4 minutes was used as a counter stain. To ensure antibody specificity, isotype controls were performed as above except that primary antibodies were replaced with rabbit IgG. Immunohistochemical staining was evaluated semiquantitatively for both percent positivity and intensity and an H-score ranging from 0 to 300 was derived on the basis of the percentage of cells stained multiplied by the intensity (0–3) of staining

Cytotoxicity assay

Cells were plated at 2,000–5,000 cells/well in 180-μL growth medium containing 10% FBS in 96-well plates, and cultured at 37°C in a humidified incubator with 5% CO_2. The following day, titrations of antibodies or ADCs in 20 μL were added and cells were incubated for 6 days. Cell viability was determined using a CellTiter-Glo Luminescent Cell Viability Assay (Promega) according to the manufacturer's instructions. A nonbinding, irrelevant negative control ADC conjugated to MMAE was also included in all assays to confirm that cell killing was antigen-dependent.

In vivo studies

Female SCID (SW-48), male SCID (Hs 746T), and SCID-Beige (NCI-H441) mice were obtained from Charles River Laboratories and housed at 10 mice per cage. The body weight upon arrival was 20–22 g. Food and water were available *ad libitum*. Mice were acclimated to the animal facilities for a period of at least one week prior to the commencement of experiments. Animals were tested in the light phase of a 12-hour light: 12-hour dark schedule (lights on at 06:00 hours). All experiments were conducted in compliance with AbbVie's Institutional Animal Care and Use Committee and the NIH Guide for Care and Use of Laboratory Animals Guidelines in a facility accredited by the Association for the Assessment and Accreditation of Laboratory Animal Care.

To generate xenografts, a suspension of viable tumors cells (SW-48: 5×10^6, NCI-H441: 5×10^6, and Hs 746T: 2×10^6) mixed with an equal amount of Matrigel (BD Biosciences) was injected subcutaneously into the flank of 6- to 8-week-old mice. The injection volume was 0.1 mL composed of a 1:1 mixture of S-MEM and Matrigel (BD Biosciences). Tumors were size matched at approximately 200–250 mm^3 unless otherwise indicated. Therapy began the day of or 24 hours after size matching the tumors. Each experimental group included 8–10 animals. Tumors were measured two to three times weekly. Measurements of the length (L) and width (W) of the tumor were obtained via electronic calipers and the volume was calculated according to the following equation: $V = L \times W^2/2$. Mice were euthanized when tumor volume reached a maximum of 3,000 mm^3 or upon presentation of skin ulcerations or other morbidities, whichever occurred first. For the LG0703 and LG1049 patient-derived xenograft (PDX) models (The Jackson Laboratory), tumor fragments of 3–5 mm^3 at passage 3 (P3) were implanted subcutaneously in the right rear flank of NOD *scid* gamma (NSG) mice (The Jackson Laboratory) with a trochar. For all groups, tumor volumes were plotted only for the duration that allowed the full set of animal to remain on study. If animals had to be taken off study, the remaining animals were monitored for tumor growth until they reached defined endpoints. Maximal tumor growth inhibition (TGI_{max}), expressed as a percentage, indicates the maximal divergence between the mean tumor volume of the test article–treated group and the control group treated with drug vehicle or isotype-matched nonbinding antibody. Tumor growth delay (TGD), expressed as a percentage, is the difference of the median time of the test article–treated group tumors to reach 1 cm^3 as compared with the control group. Complete responses (CR) were defined by tumor volume $\leq$25 mm^3 for at least three consecutive measurements. Standard-of-care agents 5-fluorouracil (50 mg/kg), and irinotecan (30 mg/kg) were administered intravenously and leucovorin (25 mg/kg) was administered orally once every 7 days for a total of five doses (FOLFIRI). IgG control, control Ig MMAE, ABBV-399, and ABT-700 were administered intraperitoneally. The carrier moiety of the control ADC represents an isotype-matched human IgG recognizing tetanus toxoid antigen that is displayed neither by the xenograft nor by murine tissue antigens.

Statistical analysis

IC_{50} and EC_{50} values were determined by nonlinear regression analysis of concentration response curves using GraphPad Prism 6.0 (GraphPad Software). Data from experiments *in vivo* were analyzed using the two-way ANOVA with *post hoc* Bonferroni correction for TGI_{max}, and the Mantel–Cox log-rank test for TGD (GraphPad Prism).

Results

Binding properties of ABBV-399 for c-Met

ABT-399 was generated by the conjugation of MMAE to the interchain cysteines of ABT-700 via a vc linker with an average drug:antibody ratio of approximately 3.1 (25). Upon binding to its target antigen on the surface of tumor cells, ABBV-399 is internalized by the cell (Supplementary Fig. S1). To confirm that the binding characteristics of the parental ABT-700 were not altered by conjugation to MMAE, both ELISA- and FACS-based assays were performed. As determined by an ELISA-binding assay to the recombinant c-Met ECD, ABBV-399 has an apparent EC_{50} of 0.30 nmol/L, comparable with that of the parent molecule, ABT-700 (Table 1). The binding affinities of ABBV-399 to surface c-Met on a panel of human cancer cells are similar to those of ABT-700 (0.2–1.5 nmol/L) by FACS (Table 1). These results indicate

Table 1. Binding affinity of ABBV-399 to recombinant and cellular c-Met

	ABBV-399 (EC_{50} nmol/L)	ABT-700 (EC_{50} nmol/L)
c-Met ECD[a] by ELISA[b]	0.30	0.22
Cellular c-Met by FACS[c]		
Hs 746T	0.4 ± 0.1	0.4 ± 0.1
SNU-5	1.4 ± 0.4	1.6 ± 1.1
IM-95	1.5 ± 0.9	1.8 ± 0.4
NCI-H820	0.2 ± 0.1	0.3 ± 0.2
NCI-H441	1.0 ± 0.6	1.1 ± 1.1
NCI-H1573	0.6 ± 0.1	0.4 ± 0.1
NCI-H1650	0.3 ± 0.2	0.4 ± 0.2

[a]Extracellular domain (residues 25-932 of c-Met).
[b]EC_{50} values derived from ELISA in which c-Met ECD was captured on the plate via a His tag. Values are the average of six experiments, ± SD.
[c]EC_{50} values derived from FACS analysis of ABBV-399 on cancer cell lines. Values are the average of at least two experiments, ± SD.

that conjugation of ABT-700 to vcMMAE does not alter the binding properties of the parental antibody.

In vitro potency of ABBV-399 against tumor cell lines and correlation with c-Met expression

To determine whether there is a correlation between c-Met expression level and sensitivity to ABBV-399, a panel of additional tumor and normal cell lines was assessed for c-Met expression and response to ABBV-399. These included NSCLC, gastroesophageal, colorectal cancer, breast, pancreatic, and glioblastoma cancer lines. FACS analysis demonstrated that these cell lines possess a range of c-Met expression levels as quantified via c-Met ABC representing the number of cell-surface c-Met molecules (Table 2). Sensitivity to ABBV-399 in the cell proliferation assay was quantified as maximal killing and IC_{50} (Table 2). The results indicated that an approximate threshold of c-Met cell surface molecules >100,000 was required for sensitivity to ABBV-399–mediated killing. Exceptions to this were the tumor cell lines known to have an autocrine HGF loop including IM-95, KP4, and U-87 MG, in which lower c-Met expression levels were sufficient for ABBV-399 to exert significant cytotoxicity (17). The differential response of some cell lines to ABBV-399 may also reflect the sensitivity of different tumor types to the auristatin payload.

ABBV-399 inhibited the proliferation of cancer cells that overexpress c-Met, including the *MET*-amplified cell lines SNU-620, SNU-5, and Hs 746T gastric cancer cells and the c-Met–overexpressed NCI-H441, EBC-1, and NCI-H820 NSCLC cell lines (Table 2). As a comparison, ABT-700 inhibited proliferation of cells with *MET* amplification but not cell lines without *MET* amplification, that is, the NCI-H820 and NCI-H441 (data not shown and 17). It is possible that ABBV-399–mediated c-Met signaling inhibition may contribute to its mechanism of action as both ABT-700 and ABBV-399 can inhibit phospho-and total c-Met and downstream signaling molecules (Supplementary Fig. S2). However, as ABBV-399 is significantly more potent than ABT-700 at lower doses and many tumor cell lines are sensitive to ABBV-399, but not to ABT-700–mediated killing, it is unlikely that signaling inhibition is a major component of ABBV-399 antitumor activity. A panel of five normal cell lines including epithelial, endothelial, and fibroblast-derived cell lines had lower levels of c-Met expression compared with the sensitive tumor cell lines and these normal cells lines were largely insensitive to ABBV-399–mediated killing (Table 2). These data suggest that that the levels of c-Met expression on normal cell lines may fall below the threshold level of c-Met expression required for significant killing by ABBV-399.

Table 2. c-Met expression on tumor cells *in vitro* and sensitivity to ABBV-399

Cell Line	c-Met Expression[a]	Maximal Killing[b]	ABBV-399 IC_{50} ± SD[c]
Lung cancer			
NCI-H1650	4,500	13%	47.9 ± 8.5
A549	43,000	22%	1.6 ± 1.1
NCI-H1573[d]	116,000	18%	18 ± 14
NCI-H441	197,000	56%	0.06 ± 0.05
EBC-1[d]	233,000	96%	0.06 ± 0.03
NCI-H820	320,000	87%	0.20 ± 0.07
Gastric cancer			
IM-95	22,000	53%	1.7 ± 0.9
SNU-620[d]	230,000	80%	0.17 ± 0.08
SNU-5[d]	291,000	85%	0.28 ± 0.07
Hs 746T[d]	350,000	87%	0.11 ± 0.06
Colorectal cancer			
SW48	26,000	0%	NA[e]
HT-29	161,000	70%	9.0 ± 1.4
Breast cancer			
MCF-7	8,000	0%	NA
MDA-MB-231	30,000	0%	NA
Pancreatic cancer			
KP4	15,000	53%	2.9 ± 1.9
Glioblastoma			
U-87 MG	22,000	30%	1.9 ± 0.1
Nontumor cell lines			
NHBE (bronchial epithelial)	40,000	10%	NA
HUVEC (vascular endothelial	16,000	6%	NA
HMEC (mammary epithelial)	ND	0%	NA
PrEC (prostate epithelial)	65,000	0%	NA
NHDF (dermal fibroblasts)	1,600	0%	NA

[a]Approximate number of c-Met molecules on cell surface determined by FACS analysis as ABC for m224G11 (the murine parent of ABT-700) binding at 10 μg/mL.
[b]Relative to untreated control at ≤1 μg/mL in a 6-day proliferation.
[c]IC_{50} values (nmol/L) for antiproliferative activity of ABBV-399 or ABT-700 in 6-day proliferation assay. Values are average of ≥2 experiments, ± the SD.
[d]*MET*-amplified cell lines (17).
[e]Not available

ABBV-399 *in vivo* efficacy in *MET*-amplified and c-Met–overexpressed tumor models

Inhibition of tumor growth by ABBV-399 was evaluated in multiple human xenograft models derived from a variety of tumor types (Table 3). Efficacy of the ADC was quantified by assessing maximal tumor growth inhibition and delayed outgrowth of tumors (tumor growth delay) following therapy in mice treated with ABBV-399 when compared with treatment with a vehicle control. Selectivity of this response was determined by comparing efficacy of a control ADC with ABBV-399.

ABBV-399 activity was compared with the parental ABT-700 antibody in the Hs 746T gastric xenograft model with amplified *MET*. One or 3 mg/kg of ABBV-399 administered once every 4 days for a total of six doses induced complete and durable tumor regression (Fig. 1A; Table 3). At the 3 mg/kg dose, 100% CRs were achieved, whereas treatment with 1 mg/kg yielded 40% CRs. ABBV-399 at 3 mg/kg was more effective than ABT-700 dosed at 10 mg/kg (Fig. 1A).

ABBV-399 also inhibited growth of NCI-H441 xenografts, a papillary lung adenocarcinoma with c-Met overexpression not caused by gene amplification (Fig. 1B; Table 3). NCI-H441

Table 3. Activity of ABBV-399 and c-Met expression in xenograft models

Xenograft	Membrane H-Score[a]	Dose (mg/kg)	TGI_{max} (%)[d]	TGD (%)[e]
Hs 746T	300	3	95	>629
NCI-H441	280	3	96	>250
EBC-1	280	3	100	>329
SW-48	40	3	65	162
LG1049[b]	170	3	NA[c]	>110
LG0703[b]	85	3	NA[c]	>53
LI0752[b]	130	6	57	129
OV250[b]	125	3	29	17

[a]H-score is a reflection of staining intensity in conjunction with percentage of cells staining positively.
[b]PDX models.
[c]Not available; cannot be calculated due to an accrual trial.
[d]Maximal tumor growth inhibition (TGI_{max}), expressed as a percentage, indicates the maximal divergence between the mean tumor volume of the test article-treated group and the control group treated with drug vehicle or isotype-matched nonbinding antibody.
[e]Tumor growth delay (TGD), expressed as a percentage, is the difference of the median time of the test article treated group tumors to reach 1 cm^3 as compared with the control group. Complete responses (CR) were defined by tumor volume $\leq$ 25 mm^3 for at least three consecutive measurements.

xenografts were eliminated (100% CR) after treatment with $\geq$1 mg/kg every 4 days for a total of six doses or higher of ABBV-399. At the same dose, ABT-700 did not significantly inhibit tumor growth. At an equivalent dose and regimen, the control IgG ADC also demonstrated no significant activity. Activity of ABBV-399 in all human xenograft models tested is summarized in Table 3 together with IHC results. These results show that ABBV-399 is most effective against models with high levels of c-Met expression.

ABBV-399 combination with chemotherapy

As clinical application of targeted therapeutics often leverage combination approaches to enhance efficacy, ABBV-399 in combination with other chemotherapies was evaluated. For these studies, SW-48 xenograft tumors derived from colorectal carcinoma were used as they had lower levels of c-Met and showed only a modest response to ABBV-399 monotherapy, providing the potential to observe combination effects (Tables 2 and 3). FOLFIRI [5-fluorouracil (5-FU), leucovorin, and irinotecan] is the standard second-line treatment for metastatic colorectal cancer (33). As shown in Fig. 1C, ABBV-399 combined with FOLFIRI had improved potency compared with either ABBV-399 or FOLFIRI alone.

Efficacy of ABBV-399 on tumors refractory to ABT-700 therapy

Efficacy of ABBV-399 was evaluated in a gastric carcinoma model (Hs 746T) that was made refractory to ABT-700 by repeated exposure to the antibody *in vivo* (Hs 746T ABT-700R). Initially, treatment of the parental Hs 746T xenografts with ABT-700 resulted in tumor stasis followed by relapse (Fig. 2A; blue line). Treatment of these relapsed tumors with ABBV-399 led to regression (Fig. 2A, red line). In contrast, Hs 746T ABT-700R xenografts were refractory to ABT-700 treatment with quick tumor outgrowth on therapy (Fig. 2B; blue line). When these refractory tumors

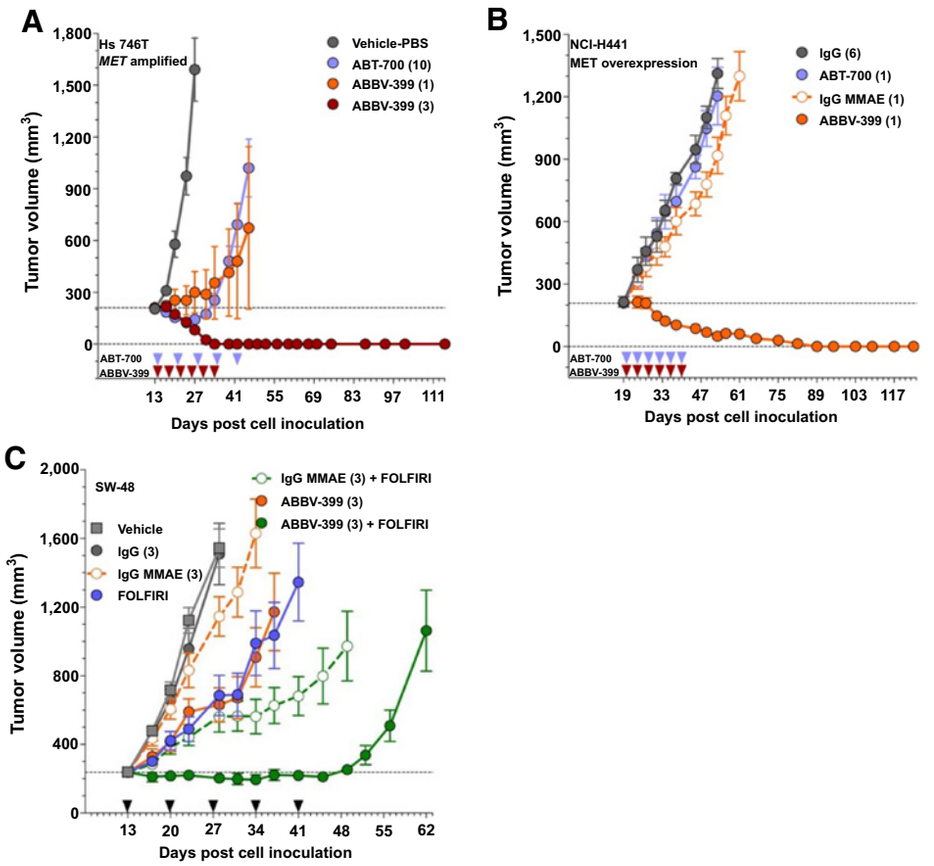

Figure 1.
ABBV-399 efficacy as monotherapy and in combination against human tumor xenograft models. The *in vivo* efficacy of ABBV-399 was evaluated in mice transplanted with Hs 746T (**A**) and NCI-H441 cells (**B**). For Hs 746T, ABT-700 was administered every 7 days while ABBV-399 was administered every 4 days. For NCI-H441 xenografts, both ABT-700 and ABBV-399 were administered every 4 days for a total of six doses. **C,** Combination efficacy of ABBV-399 and FOLFIRI was determined using SW-48 xenografts. IgG MMAE was administered as a nontargeting control agent for ABBV-399. All agents were administered every 7 days. Numbers in parentheses represent dose administered in mg/kg and arrows indicate days of administration. Administration and regimen of agents in FOLFIRI are indicated in "Materials and Methods". Tumor volumes are shown as mean ± SEM.

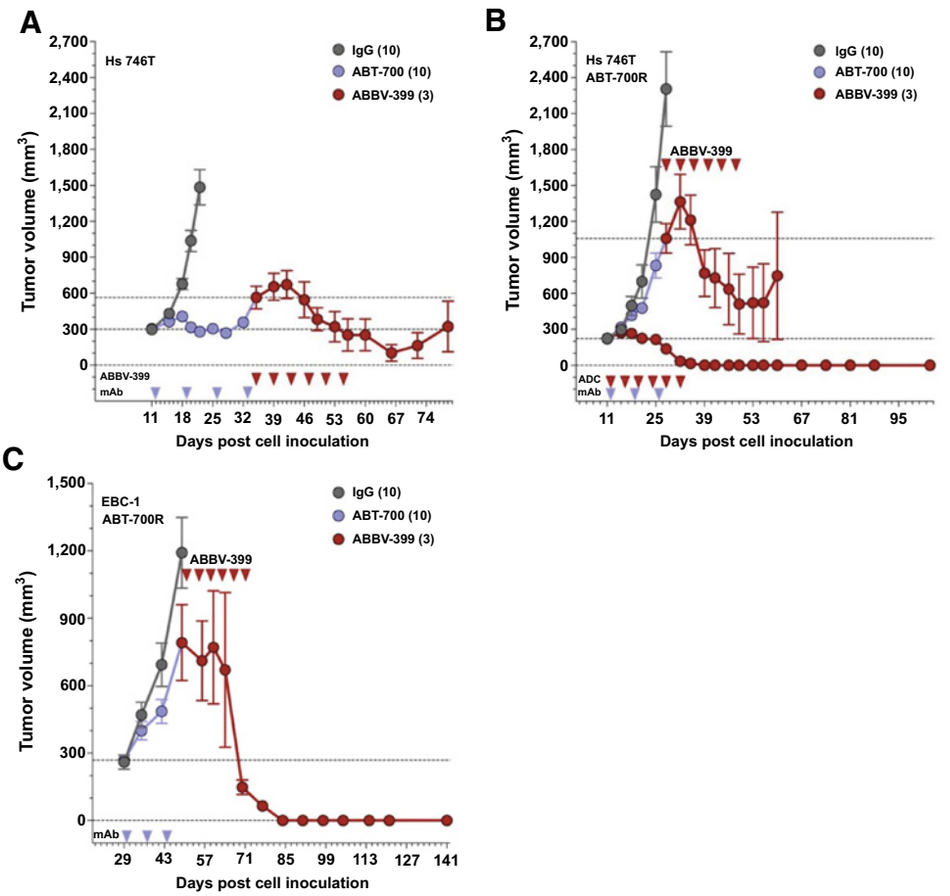

Figure 2.

ABBV-399 efficacy against human tumor xenograft models refractory to ABT-700. ABBV-399 efficacy was evaluated in mice transplanted with parental Hs 746T following relapse upon treatment with ABT-700 (**A**), Hs 746T ABT-700R as monotherapy alone or following treatment with ABT-700 (**B**), and EBC-1 ABT-700R following treatment with ABT-700 (**C**). Numbers in parentheses represent dose administered in mg/kg and arrows indicate days of administration. Tumor volumes are shown as mean ± SEM.

reached a mean cohort size of approximately 1,000 mm^3, treatment with ABBV-399 resulted in tumor regression (Fig. 2B; red line) followed by eventual outgrowth. Treatment of Hs 746T ABT-700R of approximately 200 mm^3 with ABBV-399 resulted in complete tumor regression (Fig. 2B). Similar results were observed subsequent to treatment of the ABT-700–resistant NSCLC cell line EBC-1 ABT-700R with ABT-700 followed by ABBV-399 (Fig. 2C). These results demonstrate that tumors that are no longer sensitive to c-Met pathway inhibition remain sensitive to targeted delivery of a cytotoxin with the activity of ABBV-399 independent of response to ABT-700.

Efficacy of ABBV-399 in primary PDX tumors

The antitumor activity of ABBV-399 was also evaluated in primary PDX tumors from NSCLC, hepatocellular, and ovarian carcinoma. PDX models consist of tumor fragments implanted directly from patients into immunocompromised mice and may represent a more complex model with higher heterogeneity and a closer approximation to human tumors. Because of the variable growth rate of implanted PDX tumors, these studies were performed with an accrual design with data presented as a Kaplan–Meier plot. ABBV-399 was efficacious in both lung adenocarcinoma models (LG703, LG1049) which express moderate to high levels of c-Met by IHC (Fig. 3A; Table 3). In both models the control IgG-MMAE was also active, but generally at higher doses, likely resulting from the enhanced permeability and retention effect from a combination of MMAE sensitivity and antibody accumulation in the tumor rather than the recognition of a tumor-associated antigen (34, 35). The LG1049 tumor model with the higher c-Met expression (H-score of 170 vs. H-score of 85 for LG0703) responded better to ABBV-399 treatment (Fig. 3C and D; Table 3). In the hepatocellular (LI0752) and ovarian (OV250) cancer models, both showing lower c-Met expression than the LG1049 lung model, there was a minor but statistically significant delay in tumor growth and inhibition in response to ABBV-399 treatment (Table 3).

Discussion

Development of therapeutic strategies that target c-Met activity have met with limited success. While the reasons for this are undoubtedly complex, emerging results suggest that both small-molecule and antibody c-Met inhibitors are likely to be effective primarily in those tumors that are *MET*-activated and driven predominantly by c-Met signaling (14, 15). One such example is the c-Met–targeting antibody ABT-700 which demonstrated antitumor activity only in patients with *MET*-amplified tumors (16, 17). The low frequency of *MET* amplification may limit the population responsive to this class of inhibitors. Beyond gene amplification, difficulty in identifying *MET*-activated tumors presents challenging biomarker strategies for patient selection. We describe here properties of ABBV-399 that indicate it is dependent on c-Met target expression for activity. The mechanism of action for ABBV-399 is distinct from previous c-Met inhibitors and

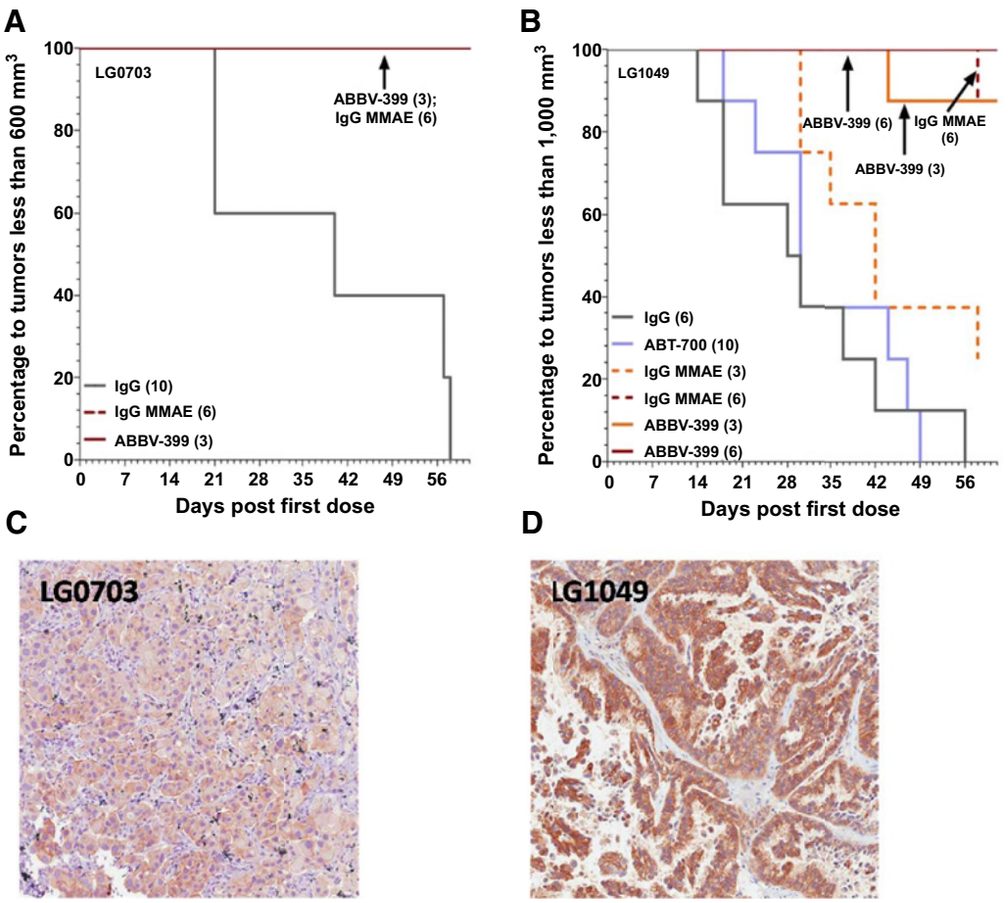

Figure 3.

ABBV-399 is active in PDX models. Efficacy of ABBV-399 was determined in xenografts derived from NSCLC patients. Efficacy is depicted on a Kaplan–Meier plot for LG0703 (**A**) and LG1049 models (**B**) as fractions reaching the indicated tumor volumes following therapy. **C** and **D,** Immunohistochemical staining for c-Met for LG0703 and LG1049 models, respectively. In both models, ABBV-399 and control agents were administered every 4 days for a total of six doses. In the LG1049 model, ABT-700 was administered every 7 days for a total of six doses. Numbers in parentheses represent dose administered in mg/kg.

suggests that ABBV-399 can overcome the limitations associated with inhibitors that are only active in *MET*-dependent tumors. ABBV-399 induces complete regressions of xenografts derived from c-Met–overexpressing or *MET*-amplified tumor cells. ABBV-399 is also effective in tumor models that are refractory to ABT-700. Extensive preclinical mouse and cynomolgus monkey pharmacokinetic studies indicate that the stability and serum clearance of ABBV-399 is comparable with the unconjugated antibody and support a once every three week dosing regimen in humans similar to that of other MMAE ADCs (26). These properties provide a sound rationale for the development of ABBV-399 as a therapeutic with the potential to be active beyond the small subgroup of patients where tumor growth is driven by c-Met signaling. In fact, in a phase I open-label study in patients with advanced solid tumors, ABBV-399 monotherapy has demonstrated durable tumor shrinkage in patients that were selected on the basis of c-Met overexpression as determined by IHC (32). The utility of IHC as a relevant companion diagnostic to identify patients most likely to respond to ABBV-399 therapy is based on the preclinical results demonstrating a strong correlation between ABBV-399 antitumor efficacy and c-Met expression levels.

A c-Met–targeting ADC presents the risk of on-target toxicity based on expression of c-Met on normal tissues including epithelial cells and hepatocytes (27) so the choice of targeting c-Met with an ADC was counterintuitive. The antitumor efficacy of ABBV-399, both *in vitro* and *in vivo*, correlated well with c-Met expression levels with tumor growth inhibition observed in both tumor cell line and primary PDXs with high c-Met expression but much less so in individual xenograft models with low c-Met expression. Consistent with the correlation of c-Met expression and sensitivity to ABBV-399, minimal inhibitory effects were observed on several c-Met–expressing normal endothelial, epithelial, and fibroblast cells. Primary toxicities observed following repeated dosing of ABBV-399 in cynomolgus monkeys were either nonadverse or reversible, consistent with those observed with other MMAE conjugates and supportive of initiation of investigational trials with this compound in humans. It is also possible that the unique properties of the parental antibody, ABT-700 targeting the immunoglobulin-like domain of the c-Met receptor may contribute to its properties as the tumor-targeting component of an ADC (36).

In a phase I clinical trial in patients with advanced solid tumors, the unconjugated ABT-700 was well tolerated at the recommended dose of 15 mg/kg (16). These clinical results together with the preclinical attributes of ABBV-399 suggest that a therapeutic window may be attainable with ABBV-399 despite the normal tissue expression profile of c-Met. This premise is supported by results of the ABBV-399 phase I expansion cohort indicating that ABBV-399 is well tolerated at a dose of 2.7 mg/kg (32). As a point of reference, the recommended clinical dose for Adcetris (brentuximab vedotin), an FDA-approved antibody drug conjugated with MMAE, is 1.8 mg/kg every 3 weeks (26).

The tolerability of ABBV-399 monotherapy in clinical studies coupled with preclinical results showing improved potency in combination with chemotherapy also suggests the potential for ABBV-399 combination therapy. Combination treatments may enhance efficacy and forestall or prevent the emergence of drug resistance. The precedence for ADC combination with chemotherapy is increasingly being established as a viable treatment option (37). Strategies combining ABBV-399 with immunotherapy agents that activate the immune system could also represent a promising treatment option. There exists a strong rationale for this combination as microtubule inhibitor–based ADCs have been shown to induce dendritic cell homing to tumor draining lymph nodes and augment host immunity in preclinical models (38).

In summary, ABBV-399 is a novel c-Met–targeted therapy that may overcome limitations that have adversely influenced clinical development of other c-Met inhibitors. Continued assessment of ABBV-399, both as monotherapy and in combination across a broad range of c-Met–expressing tumors is warranted.

Disclosure of Potential Conflicts of Interest

M.G. Anderson has ownership interest (including patents) in AbbVie. No potential conflicts of interest were disclosed by the other authors.

Authors' Contributions

Conception and design: J. Wang, M.G. Anderson, K.S. Vaidya, E.R. Boghaert, J.P. Palma, L. Naumovski, E.B. Reilly

Development of methodology: J. Wang, M.G. Anderson, A. Oleksijew, L. Tucker, Q. Zhang

Acquisition of data (provided animals, acquired and managed patients, provided facilities, etc.): M.G. Anderson, A. Oleksijew, K.S. Vaidya, L. Tucker, Q. Zhang, J.P. Palma

Analysis and interpretation of data (e.g., statistical analysis, biostatistics, computational analysis): J. Wang, M.G. Anderson, K.S. Vaidya, B. Erwin, L. Tucker, Q. Zhang, E.K. Han, J.P. Palma, L. Naumovski, E.B. Reilly

Writing, review, and/or revision of the manuscript: J. Wang, M.G. Anderson, A. Oleksijew, K.S. Vaidya, B. Erwin, L. Tucker, Q. Zhang, E.K. Han, J.P. Palma, L. Naumovski, E.B. Reilly

Administrative, technical, or material support (i.e., reporting or organizing data, constructing databases): E.B. Reilly

Study supervision: J. Wang, M.G. Anderson, A. Oleksijew, K.S. Vaidya, B. Erwin, L. Naumovski, E.B. Reilly

Acknowledgments

The authors thank Dr. Sasmita Mishra, Dr. Cherrie Donawho, Jerry Clarin, and Sally Schlessinger for assistance with IHC, Dr. Neal Goodwin (Champions Oncology) for providing the PDX models, and Dr. Andrew Phillips for manuscript review.

The costs of publication of this article were defrayed in part by the payment of page charges. This article must therefore be hereby marked *advertisement* in accordance with 18 U.S.C. Section 1734 solely to indicate this fact.

Received June 21, 2016; revised August 4, 2016; accepted August 10, 2016; published OnlineFirst August 29, 2016.

References

1. Gherardi E, Birchmeier W, Birchmeier C, Vande Woude G. Targeting MET in cancer: rationale and progress. Nat Rev Cancer 2012;12:89–103.
2. Liu X, Newton RC, Scherle PA. Developing c-MET pathway inhibitors for cancer therapy: progress and challenges. Trends Mol Med 2010;16:37–45.
3. Cecchi F, Rabe DC, Bottaro DP. Targeting the HGF/Met signalling pathway in cancer. Eur J Cancer 2010;46:1260–70.
4. Peters S, Adjei AA. MET: a promising anticancer therapeutic target. Nat Rev Clin Oncol 2012;9:314–26.
5. Pietronave S, Forte G, Locarno D, Merlin S, Zamperone A, Nicotra G, et al. Agonist monoclonal antibodies against HGF receptor protect cardiac muscle cells from apoptosis. Am J Physiol Heart Circ Physiol 2010;298:H1155–65.
6. Prat M, Crepaldi T, Pennacchietti S, Bussolino F, Comoglio PM. Agonistic monoclonal antibodies against the Met receptor dissect the biological responses to HGF. J Cell Sci 1998;111(Pt 2):237–47.
7. Jin H, Yang R, Zheng Z, Romero M, Ross J, Bou-Reslan H, et al. MetMAb, the one-armed 5D5 anti-c-Met antibody, inhibits orthotopic pancreatic tumor growth and improves survival. Cancer Res 2008;68:4360–8.
8. Patnaik A, Weiss GJ, Papadopoulos KP, Hofmeister CC, Tibes R, Tolcher A, et al. Phase I ficlatuzumab monotherapy or with erlotinib for refractory advanced solid tumours and multiple myeloma. Br J Cancer 2014;111:272–80.
9. Jun HT, Sun J, Rex K, Radinsky R, Kendall R, Coxon A, et al. AMG 102, a fully human anti-hepatocyte growth factor/scatter factor neutralizing antibody, enhances the efficacy of temozolomide or docetaxel in U-87 MG cells and xenografts. Clin Cancer Res 2007;13(22 Pt 1):6735–42.
10. Ou SH, Kwak EL, Siwak-Tapp C, Dy J, Bergethon K, Clark JW, et al. Activity of crizotinib (PF02341066), a dual mesenchymal-epithelial transition (MET) and anaplastic lymphoma kinase (ALK) inhibitor, in a non-small cell lung cancer patient with de novo MET amplification. J Thorac Oncol 2011;6:942–6.
11. Yakes FM, Chen J, Tan J, Yamaguchi K, Shi Y, Yu P, et al. Cabozantinib (XL184), a novel MET and VEGFR2 inhibitor, simultaneously suppresses metastasis, angiogenesis, and tumor growth. Mol Cancer Ther 2011;10:2298–308.
12. Yap TA, Olmos D, Brunetto AT, Tunariu N, Barriuso J, Riisnaes R, et al. Phase I trial of a selective c-MET inhibitor ARQ 197 incorporating proof of mechanism pharmacodynamic studies. J Clin Oncol 2011;29:1271–9.
13. Aoyama A, Katayama R, Oh-Hara T, Sato S, Okuno Y, Fujita N. Tivantinib (ARQ 197) exhibits antitumor activity by directly interacting with tubulin and overcomes ABC transporter-mediated drug resistance. Mol Cancer Ther 2014;13:2978–90.
14. Sheridan C. Genentech to salvage anti-MET antibody with subgroup analysis. Nat Biotechnol 2014;32:399–400.
15. Garber K. MET inhibitors start on road to recovery. Nat Rev Drug Discov 2014;13:563–5.
16. Strickler JH, LoRusso P, Yen C-J, Lin C-C, Kang Y-K, Kaminker P, et al. Phase 1, open-label, dose-escalation, and expansion study of ABT-700, an anti-C-met antibody, in patients (pts) with advanced solid tumors. J Clin Oncol 32:5s, 2014 (suppl; abstr 2507).
17. Wang J, Goetsch L, Tucker L, Zhang Q, Gonzalez A, Vaidya KS, et al. Anti-c-Met monoclonal antibody ABT-700 breaks oncogene addiction in tumors with MET amplification. BMC Cancer 2016;16:105.
18. Nakajima M, Sawada H, Yamada Y, Watanabe A, Tatsumi M, Yamashita J, et al. The prognostic significance of amplification and overexpression of c-met and c-erb B-2 in human gastric carcinomas. Cancer 1999;85:1894–902.
19. Zeng ZS, Weiser MR, Kuntz E, Chen CT, Khan SA, Forslund A, et al. c-Met gene amplification is associated with advanced stage colorectal cancer and liver metastases. Cancer Lett 2008;265:258–69.
20. Engelman JA, Zejnullahu K, Mitsudomi T, Song Y, Hyland C, Park JO, et al. MET amplification leads to gefitinib resistance in lung cancer by activating ERBB3 signaling. Science 2007;316:1039–43.

21. Bean J, Brennan C, Shih JY, Riely G, Viale A, Wang L, et al. MET amplification occurs with or without T790M mutations in EGFR mutant lung tumors with acquired resistance to gefitinib or erlotinib. Proc Natl Acad Sci U S A 2007;104:20932–7.
22. Spigel DR, Ervin TJ, Ramlau RA, Daniel DB, Goldschmidt JH Jr, Blumenschein GR Jr, et al. Randomized phase II trial of Onartuzumab in combination with erlotinib in patients with advanced non-small-cell lung cancer. J Clin Oncol 2013;31:4105–14.
23. Resnick MB, Routhier J, Konkin T, Sabo E, Pricolo VE. Epidermal growth factor receptor, c-MET, beta-catenin, and p53 expression as prognostic indicators in stage II colon cancer: a tissue microarray study. Clin Cancer Res 2004;10:3069–75.
24. Lee HE, Kim MA, Lee HS, Jung EJ, Yang HK, Lee BL, et al. MET in gastric carcinomas: comparison between protein expression and gene copy number and impact on clinical outcome. Br J Cancer 2012;107:325–33.
25. Doronina SO, Toki BE, Torgov MY, Mendelsohn BA, Cerveny CG, Chace DF, et al. Development of potent monoclonal antibody auristatin conjugates for cancer therapy. Nat Biotechnol 2003;21:778–84.
26. Okeley NM, Alley SC, Senter PD. Advancing antibody drug conjugation: from the laboratory to a clinically approved anticancer drug. Hematol Oncol Clin North Am 2014;28:13–25.
27. Di Renzo MF, Narsimhan RP, Olivero M, Bretti S, Giordano S, Medico E, et al. Expression of the Met/HGF receptor in normal and neoplastic human tissues. Oncogene 1991;6:1997–2003.
28. Brinkmann V, Foroutan H, Sachs M, Weidner KM, Birchmeier W. Hepatocyte growth factor/scatter factor induces a variety of tissue-specific morphogenic programs in epithelial cells. J Cell Biol 1995;131(6 Pt 1):1573–86.
29. Tsarfaty I, Resau JH, Rulong S, Keydar I, Faletto DL, Vande Woude GF. The met proto-oncogene receptor and lumen formation. Science 1992;257:1258–61.
30. Schmidt C, Bladt F, Goedecke S, Brinkmann V, Zschiesche W, Sharpe M, et al. Scatter factor/hepatocyte growth factor is essential for liver development. Nature 1995;373:699–702.
31. Nusrat A, Parkos CA, Bacarra AE, Godowski PJ, Delp-Archer C, Rosen EM, et al. Hepatocyte growth factor/scatter factor effects on epithelia. Regulation of intercellular junctions in transformed and nontransformed cell lines, basolateral polarization of c-met receptor in transformed and natural intestinal epithelia, and induction of rapid wound repair in a transformed model epithelium. J Clin Invest 1994;93:2056–65.
32. Strickler J, Nemunaitis J, Weekes C, Ramanathan RK, Angevin E, Morgensztern D, et al. Phase 1, open-label, dose-escalation and expansion study of ABBV-399, an antibody drug conjugate (ADC) targeting c-Met, in patients (pts) with advanced solid tumors. J Clin Oncol 34, 2016 (suppl; abstr 2510).
33. Tournigand C, Andre T, Achille E, Lledo G, Flesh M, Mery-Mignard D, et al. FOLFIRI followed by FOLFOX6 or the reverse sequence in advanced colorectal cancer: a randomized GERCOR study. J Clin Oncol 2004;22:229–37.
34. Boghaert ER, Khandke K, Sridharan L, Armellino D, Dougher M, Dijoseph JF, et al. Tumoricidal effect of calicheamicin immuno-conjugates using a passive targeting strategy. Int J Oncol 2006;28:675–84.
35. Fang J, Nakamura H, Maeda H. The EPR effect: Unique features of tumor blood vessels for drug delivery, factors involved, and limitations and augmentation of the effect. Adv Drug Deliv Rev 2011;63:136–51.
36. Gonzalez A, Broussas M, Beau-Larvor C, Haeuw JF, Boute N, Robert A, et al. A novel antagonist anti-cMet antibody with antitumor activities targeting both ligand-dependent and ligand-independent c-Met receptors. Int J Cancer 2016;139:1851–63.
37. Diamantis N, Banerji U. Antibody-drug conjugates-an emerging class of cancer treatment. Br J Cancer 2016;114:362–7.
38. Muller P, Martin K, Theurich S, Schreiner J, Savic S, Terszowski G, et al. Microtubule-depolymerizing agents used in antibody-drug conjugates induce antitumor immunity by stimulation of dendritic cells. Cancer Immunol Res 2014;2:741–55.